

REPORT DOCUMENTATION PAGE

AFRL-SR-AR-TR-04-

Public reporting burden for this collection of information is estimated to average 1 hour per response, including gathering and maintaining the data needed, and completing and reviewing the collection of information. Send collection of information, including suggestions for reducing this burden, to Washington Headquarters Services, Directorate for Information Operations and Reports, 1215 Jefferson Davis Highway, Suite 1204, Arlington, VA 22202-4302, and to the Office of Management and Budget, Paperwork Project, Washington, DC 20503.

S,
is
in

0467

1. AGENCY USE ONLY (Leave blank)	2. REPORT DATE	3. REPORT TYPE AND DATES COVERED 01 Feb 2001 - 31 Jan 2004 FINAL	
4. TITLE AND SUBTITLE (THEME 2) Generation Characterization and Aerospace Application of Torch Plasmas		5. FUNDING NUMBERS 61102F 2308/TA	
6. AUTHOR(S) Dr Kuo			
7. PERFORMING ORGANIZATION NAME(S) AND ADDRESS(ES) POLYTECHNIC UNIVERSITY SIX METROTECH CENTER BROOKLYN NY 11201		8. PERFORMING ORGANIZATION REPORT NUMBER	
9. SPONSORING/MONITORING AGENCY NAME(S) AND ADDRESS(ES) AFOSR/NE 4015 WILSON BLVD SUITE 713 ARLINGTON VA 22203		10. SPONSORING/MONITORING AGENCY REPORT NUMBER F49620-01-1-0392	

11. SUPPLEMENTARY NOTES

12a. DISTRIBUTION AVAILABILITY STATEMENT
DISTRIBUTION STATEMENT A: Unlimited

20040914 015

13. ABSTRACT (Maximum 200 words)
This basic research effort addressed the physical issues related to the generation of atmospheric pressure plasmas and to the use of "Torch Plasmas" for aerospace applications. The most significant accomplishment has been the development of a plasma torch into an ignition aide for use in scramjet engines. It was shown that such a torch can deliver sufficient heat to cold, liquid JP-7 fuel injected into a Mach-2 crossflow (having a static temperature of ~ 500 K) to reduce the ignition delay time and to increase the rate of combustion and, thus, to initiate main-duct combustion.

14. SUBJECT TERMS		15. NUMBER OF PAGES	
		16. PRICE CODE	
17. SECURITY CLASSIFICATION OF REPORT Unclassified	18. SECURITY CLASSIFICATION OF THIS PAGE Unclassified	19. SECURITY CLASSIFICATION OF ABSTRACT Unclassified	20. LIMITATION OF ABSTRACT UL

BEST AVAILABLE COPY

Final Report on Air Force Office of Scientific Research Grant

AFOSR- F49620-01-1-0392

(June 1, 2001 – May 31, 2004)

**Generation, Characterization, and Aerospace Applications of
Torch Plasmas**

Professor Spencer P. Kuo, Principal Investigator

Dr. Daniel Bivolaru, Research Scientist

Henry Lai, Graduate Student

Wilson Lai, Graduate Student

Department of Electrical & Computer Engineering

Polytechnic University

6 Metrotech Center

Brooklyn, NY 11201

DISTRIBUTION STATEMENT A
Approved for Public Release
Distribution Unlimited

I. Introduction

The present report summarizes the work, under the support of the AFOSR Grant AFOSR-F49620-01-1-0392, conducted during the period from June 1, 2001 to May 31, 2004. This research program carried out basic research on the physical issues related to the generation of atmospheric pressure plasmas and to explore the engineering merits of "Torch Plasmas" for aerospace applications.

Plasmas in most of aerospace applications are required to be exposed directly to the atmosphere. Therefore, there are considerable interests in the development of plasma sources having open structures. Most of the applications also require plasmas to be dense and in large volumes. Dense atmospheric-pressure plasma can be produced through dc or low frequency discharge operating in the high current diffused arc mode, such as a plasma torch^{1,2}, which introduces a gas flow to carry the plasma out of the discharge region. The inertia of the gas flow carries the plasma to give rise a longer discharge current path, which increases the plasma volume as well as lifetime, and thus, reduces the power budget considerably. The volume of a single torch is generally restricted by the gap between the electrodes, which is, in turn, limited by the available voltage of the power supply. A simple way to enlarge the plasma volume is to light an array of torches simultaneously². The torches in an array can be arranged to couple to each other, for example, through capacitors. In doing so, the number of power sources needed to operate the array can be reduced considerably, so that the size of the power supply can be compact for the practical reason. The installation of an array of plasma torches is made easy by introducing a cylindrical-shape plasma torch module^{3,4} as a building block, which simplifies the design of a large volume plasma source and also makes easy to the maintenance of the source. Different aerospace applications require different plasma characteristics. For example, plasma rampart application prefers low-temperature and high-density plasma in large volume⁵; on the other hand, high-energy plasma jet is required to be an effective igniter in the scramjet engine⁶⁻⁹. For the mitigation of shock wave, plasma has to be generated symmetrically in front of the shock front¹⁰.

Among the works that have been accomplished, the development of a plasma torch into an ignition aide in the scramjet engine is the most noticeable effort. For the

hydrocarbon-fueled scramjet in a typical startup scenario, cold liquid JP-7 is injected into a Mach-2 air crossflow (having a static temperature of ~ 500 K); under these conditions, the fuel-air mixture will not auto-ignite. Thus some ignition aide, for example, plasma torches that can deliver enough heat to the mixture to reduce the ignition delay time and to increase the rate of combustion, is necessary to initiate main-duct combustion.

In November 2002, experiments to study the ignition of hydrocarbon fuel by our 60-Hz torch plasma have been conducted in a supersonic (Mach-2) flow facility, at Wright-Patterson Air Force Research Laboratory. The experiment was carried out jointly with Cam Carter, Lance Jacobsen, and Skip Williams of AFRL. This scramjet test cell in Wright-Patterson is capable of heating the air to about 750 K and does not include a cavity-based flame-holder in the simulated scramjet combustor duct. Tests have been conducted using gaseous ethylene fuel with the 15-deg downstream-angled single-hole and aero-ramp injectors. Substantial flame plume has been observed. This is illustrated in Fig. 1.1, which shows two still shots from video recordings of flame plumes having fuel injected by (a) single-hole injector and (b) aero-ramp injector.

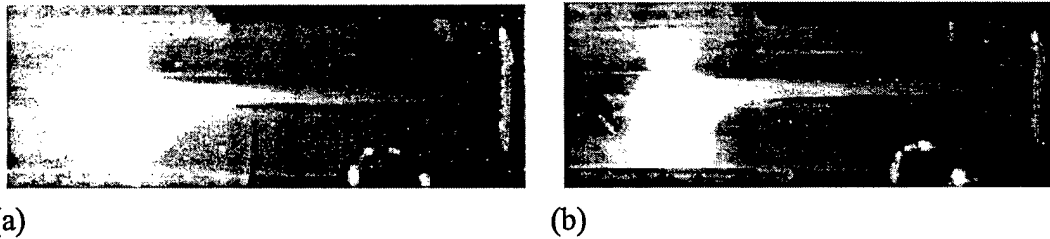


Fig. 1.1 Flame plume ignited by 60-Hz torch plasma with fuel injected by (a) single-hole injector and (b) aero-ramp injector.

The experimental results showed that our air plasma torch ignited a stoichiometric C_2H_4/O_2 mixture at Mach 2.5. Torch plasma penetrated deeply into the combustor as anticipated. This advantageous feature offers nonlocal ignition, which helps to reduce the ignition delay.

II. Publications from the Work Sponsored by this AFOSR Grant (AFOSR-F49620-01-1-0392)

Journal Papers:

1. S. P. Kuo and Daniel Bivolaru, "Plasma effect on shock waves in a supersonic flow", Phys. Plasmas, 8 (7), 3258-3264, 2001.
2. Daniel Bivolaru and S. P. Kuo, "Observation of supersonic wave mitigation by plasma aero-spike", Phys. Plasmas, 9(2), 721-723, 2002.
3. S. P. Kuo, D. Bivolaru, and Lester Orlick, "A magnetized torch module for plasma generation", Rev. Sci. Instruments, 73(8), 3119-3121, 2002.
4. S. P. Kuo and Daniel Bivolaru, "Electric discharge in the presence of supersonic shocks", Phys. Lett. A, 313(1-2), 101-105, 2003.
5. S. P. Kuo, Daniel Bivolaru, Campbell D. Carter, Lance Jacobsen, and Skip Williams, "Operational Characteristics of a Periodic Plasma Torch", IEEE Trans. Plasma Sci., 32 (1), 262-268, 2004.
6. S. P. Kuo, "Conditions and a physical mechanism for plasma mitigation of shock wave in a supersonic flow", Physica Scripta, 70, 161-165, 2004.
7. S. P. Kuo, D. Bivolaru, H. Lai, W. Lai, S. Popovic and P. Kessaratikoon, "Characteristics of An Arc-seeded Microwave Plasma Torch", IEEE Trans. Plasma Sci., August Issue, 2004.
8. Daniel Bivolaru and S. P. Kuo, "Aerodynamic Modification of supersonic flow around truncated cone using Pulsed Electrical Discharges", submitted to AIAA Journal.

Proceedings articles:

1. S. P. Kuo, D. Bivolaru, and Lester Orlick, "A magnetized torch module for plasma generation and plasma diagnostic with microwave", AIAA Paper 2003-135, American Institute of Aeronautics and Astronautics, Washington DC, Jan. 2003.
2. S. P. Kuo and Daniel Bivolaru, "A physical mechanism of the plasma effect on shock waves", AIAA Paper 2003-527, American Institute of Aeronautics and Astronautics, Washington DC, Jan. 2003.

3. S. P. Kuo, Daniel Bivolaru, Campbell D. Carter, Lance Jacobsen, and Skip Williams, "Operational characteristics of a plasma torch in a supersonic cross flow", *AIAA Paper 2003-1190*, American Institute of Aeronautics and Astronautics, Washington DC, Jan. 2003.
4. S. P. Kuo, Daniel Bivolaru, Henry Lai, and Wilson Lai, and S. Popovic, "Plasma torch igniters for a scramjet combustor", *AIAA Paper 2004-839*, American Institute of Aeronautics and Astronautics, Washington DC, Jan. 2004.
5. Skip Williams et al., "Model Development for Plasma Assisted Combustion", *AIAA Paper 2004-1012*, American Institute of Aeronautics and Astronautics, Washington DC, Jan. 2004.
6. D. Bivolaru and S. P. Kuo, "On-Board Generated Plasma for Supersonic Flow Study", *AIAA Paper 2004-675*, American Institute of Aeronautics and Astronautics, Washington DC, Jan. 2004.

C. Articles in a Book "Non-Equilibrium Air Plasmas at Atmospheric Pressure", ed. by R. Barker, K. Becker, and K. Schoenbach, Institute of Physics Publishing, 2004.

1. S. P. Kuo, "Operational Characteristics of a Low Temperature AC Plasma Torch".
2. S. P. Kuo, "Methods for Spatial Localization of a Microwave Discharge".
3. S. P. Kuo, "The Plasma Mitigation of the Shock Waves in Supersonic/Hypersonic Flights".
4. S. P. Kuo, "Plasma Torch for Enhancing Hydrocarbon-Air Combustion in the Scramjet Engine".

D. Conference Presentations:

1. S. P. Kuo, D. Bivolaru, and E. Koretzky, "Density and temperature measurements of torch plasma", *Icops2002, 02CH37340, Paper # 5P31, p. 272.*
2. S. P. Kuo, D. Bivolaru, and Lester Orlick "A magnetized torch module for plasma generation", *Icops2002, 02CH37340, Paper # 1P17, p. 116.*
3. Daniel Bivolaru and S. P. Kuo, "Evidence of non-thermal plasma effect for supersonic drag reduction", *Icops2002, 02CH37340, Paper # 5A07, p. 242.*

4. E. Koretzky and S. P. Kuo, "Simulation Study of a Capacitive-Coupled Plasma Torch Array", Icops2002, 02CH37340, Paper # 2C07, p. 136.

Ph.D Dissertation:

1. Daniel Bivolaru, "On the use of plasma for shock wave mitigation," Ph. D. dissertation, Polytechnic University, May 2002.

MS Dissertations:

1. Henry Lai, E.E., June 2004, "Design and Study of A Microwave-augmented Plasma Torch - Igniter for Supersonic Combustor."
2. Wilson Lai, E.E., June 2004, "A Portable Arc-seeded Microwave Plasma Torch and Its Application for Decontamination of Biological Warfare Agents."

III. Summary of Work Accomplished

A brief description of results of the research effort is given in the following. The published articles have been or will be sent to the program manager Dr. Barker by the regular mail for providing detail description of accomplished works.

1. Plasma effect on shock waves in a supersonic flow

An experimental study of the plasma effect on the structure of an attached conical shock front appearing at the front end of a cone-shaped model has been carried out in a Mach 2.5 stream. The tip and the body of the model are designed as the cathode and anode, which are separated by a conical-shaped ceramic insulator providing a 5-mm gap for gaseous discharge. The tip is shaped to match the cone angle of the wind tunnel model. It turns out that the sharp tip also works to enhance the electric field intensity in the region in front of the tip. Moreover, the tip of the model is arranged as the cathode. This arrangement together with the favorable electric field distribution make electron current in the discharge much easier to pass through the shock front into the upstream (lower pressure) region before returning to the body of the model as the anode. Plasma produced by the electric discharge in the upstream region can have a symmetric distribution around the tip as seen by its airglow image shown in Fig. 3.1.1a.

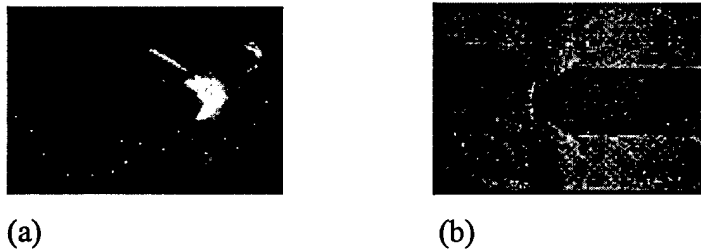


Fig. 3.1.1 (a) Plasma produced in front of the model with a symmetric distribution around the tip of the model and (b) the shadowgraph of the flow field showing strong plasma effect on shock wave.

It is observed that such plasma can cause shock wave to move upstream with its shock front detached from the model. The shock front is also becoming more and more diffusive and having an increasing shock angle as seen in a shadow video graph of the flow presented in Fig. 3.1.1b. A physical mechanism of the observed plasma effect on this type of shock wave is also presented.

2. Observation of supersonic shock wave mitigation by a plasma aero-spike

A wind tunnel model in the shape of a 30° half-angle truncated cone is designed to generate a strong bow shock behind a weak Mach wave, attached to the tip of a protruding central-electrode, in a non-ionized supersonic flow as shown in Fig. 3.2.1a. This model is also facilitated with an on-board discharge arrangement to produce plasma between two waves as shown in Fig. 3.2.1b. The result presented in Fig. 3.2.1c demonstrates that the introduced plasma spike can drastically modify the original complicated shock structure shown in Fig. 3.2.1a to the simple structure of a single conical shock shown in Fig. 3.2.1c. A significant drag reduction in each discharge was measured; the result as presented in Fig. 3.2.2 indicates that this plasma spike reduced energy loss more than the applied electric pulse energy, leading to a net energy saving. The measurements also showed that the gas temperature increase near the cone surface was less than 10 % during the discharge and the plasma effect on shock structure lasted much longer than the discharge period.

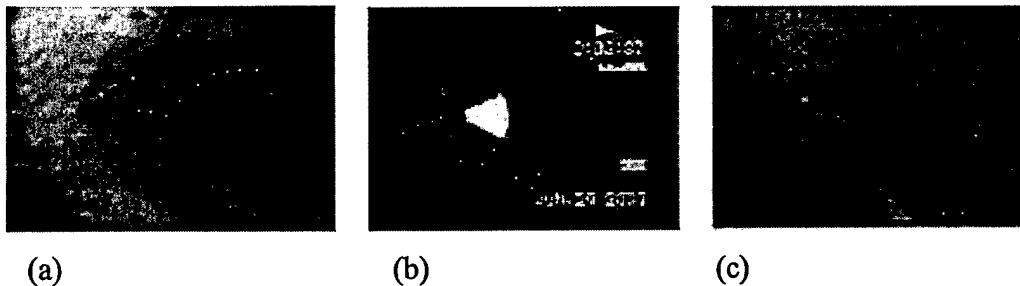


Fig. 3.2.1 (a) A baseline Schlieren image of the flowfield in the absence of plasma; (b) Cone-shaped plasma as a plasma spike produced in front of the nose of the model with a symmetric distribution around the physical spike and (c) a Schlieren image of the flowfield in the presence of the plasma spike showing strong plasma effect on shock wave.

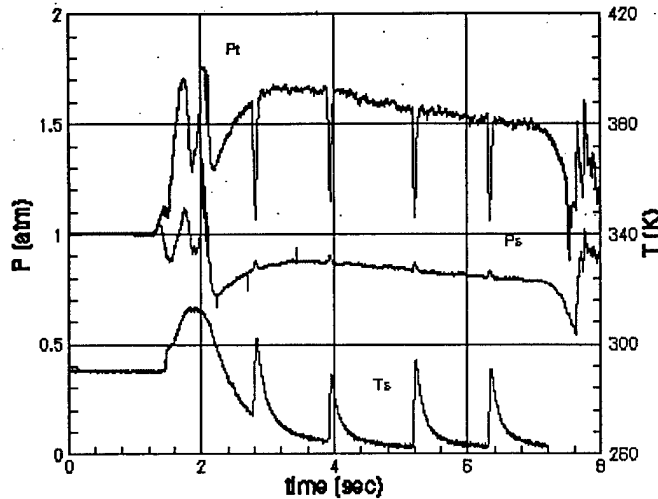
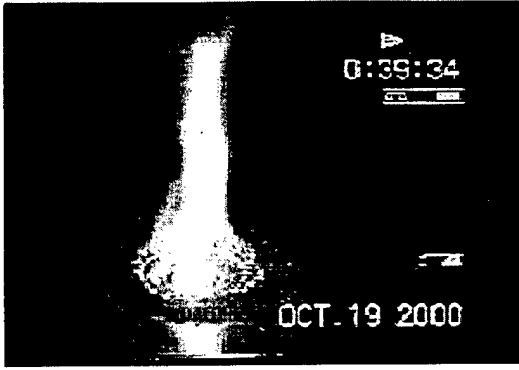


Fig. 3.2.2 Pressure measurements (top and middle plots using the vertical scale to the left side) by transducers placed on the frontal and cone surfaces of the model; temperature measurement (bottom plot using the vertical scale to the right side) by a thermocouple probe placed on the cone surface.

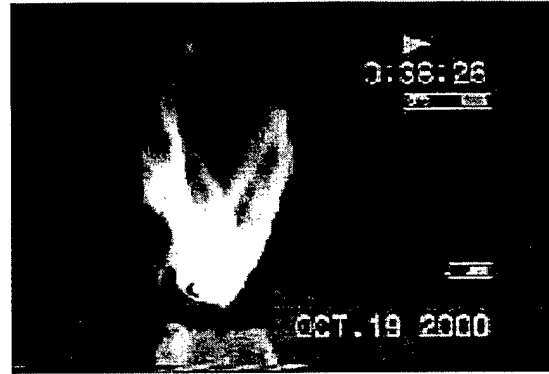
3. A magnetized torch module for plasma generation

Remodeling components from two commercially available spark plugs and adding tungsten wire as the central electrode construct a cylindrical-shape magnetized plasma torch module. A ring-shaped permanent magnet is used to provide an axial magnetic field. This magnetic field is in the (axial) direction perpendicular to the discharge electric field (in the radial direction). It rotates the discharge by the $\mathbf{J} \times \mathbf{B}$ force around the electrodes (in the azimuth direction) and thus, enhances the strength (e.g., density and allowable gas flow speed) and stability (e.g., of the shape) of plasma produced by the module, and the lifetime of the electrodes by avoiding discharge at a fixed hot spot. Shown in Fig. 3.3.1a is a photo of torch plasma produced by this new module. A photo of unmagnetized torch plasma is presented in Fig. 3.3.1b for comparison. The first noticeable difference between these two is their sizes. The volume of magnetized torch plasma is evidently larger. The evenly distributed bright spots around the base of magnetized torch demonstrate the rotation of the discharge by the magnetic field, which helps to optimize the torch volume. The electric properties of this magnetized torch module are studied and compared with those of the unmagnetized one.

This module is designed as a unit of a torch array for plasma generation. An array of four torches is demonstrated in Fig. 3.3.2.



(a)



(b)

Fig. 3.3.1 Torch plasma produced by (a) a magnetized and (b) an unmagnetized torch module.

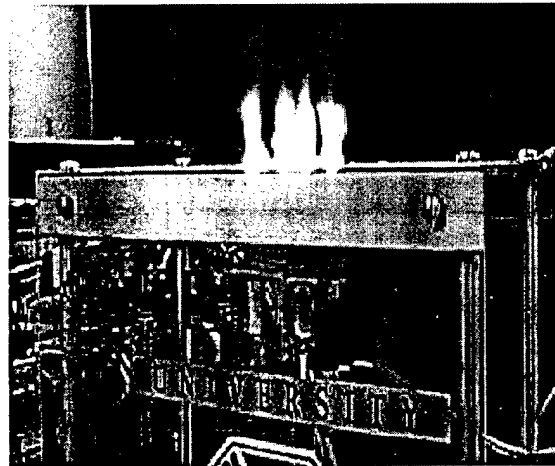


Fig. 3.3.2 A photo of four plasma torches produced by a portable array.

4. Electric discharge in the presence of supersonic shocks

A cone-shaped shock wave generator is placed in a Mach 2.5 flow to generate a conic shock attached to its tip. The interaction of on-board 60 Hz pulsed discharge with this shock wave is investigated by means of the spatial distribution and temporal evolution of discharge-induced airglow imaging.

During several wind tunnel runs we observed the destabilization of the flow by the introduced plasma. The shadowgraph in Fig. 3.4.1a shows the appearance of a diamond shock during the run, while shock wave in front of the model is being strongly perturbed by plasma. In the graph, the flow is from left to right. In the absence of plasma,

the upstream flow (in front of the unperturbed shock waves) had a flow speed $v = 570$ m/s and a pressure $p_1 = 1.8 \times 10^4$ N/m². This diamond shock structure moves downstream, as shown in the subsequent three shadowgraphs presented in Figs. 3.4.1b to d. This sequence of shadowgraphs also shows that shock wave in front of the model starts to recover after the diamond shock has passed the tip of the model.

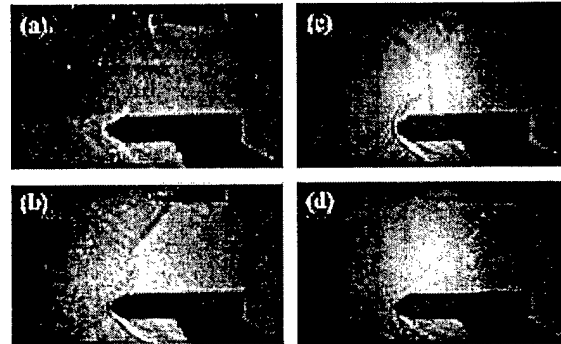


Fig. 3.4.1 A sequence of shadowgraphs showing sudden appearance of a diamond shock and its temporal evolution during a wind tunnel run. (a) A diamond shock is formed in the upstream region while the shock wave in front of the model is severely perturbed by the plasma, and (b) to (d) diamond shock has passed the tip of the model and the shock wave in front of the model is recovering.

Because the discharge was conducted in the region where shock wave appeared, the stability of the flow together with the temporal variation of the shock wave structure were expected to have a strong influence on the discharge. Indeed, as expected when the flow became unstable due to the plasma perturbation, the oscillation of the shock front position could also destabilize the discharge, as observed in the airglow images recorded by the video camera during the runs. The manifestation of relaxation instability in the discharge is exposed in Fig. 3.4.2 by a consecutive time sequence of eight video graphs showing two cycles of the temporal evolution of the discharge. In the first cycle covered by Figs. 3.4.2a to d, the discharge starts with constricted arcs (Fig. 3.4.2a). This constricted arc mode suddenly changes to a glow mode producing a diffused glow (Fig. 3.4.2b), which then evolves back to constricted arc mode (Fig. 3.4.2d) through a diffused arc-glow transition (Fig. 3.4.2c). Figs. 3.4.2e to h repeat the cycle of the discharge starting from a diffused glow (Fig. 3.4.2e) and changed suddenly to constricted arcs (Fig.

3.4.2f), which then evolve through a diffused arc-glow transition (Fig. 3.4.2g) back to a diffused glow (Fig. 3.4.2h).

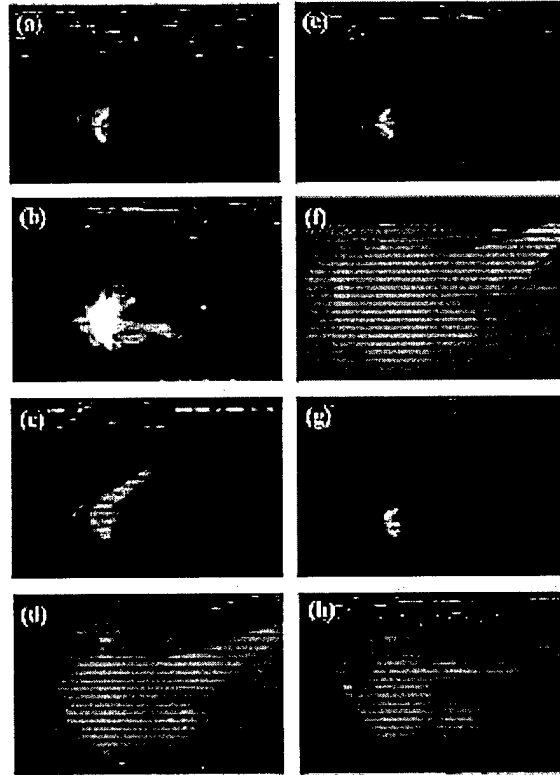


Fig. 3.4.2 Relaxation instability in the discharge. (a) to (e) A cycle showing that the discharge evolves from constricted arcs to a big diffused glow, and then evolves back to constricted arcs through a glow-diffused arc transition, and (e) to (h) showing a repeating one and half cycles of the evolution of the discharge.

5. Operational Characteristics of a Periodic Plasma Torch

Development of a plasma torch, which is intended as an ignition aid within a supersonic-combustor, is studied. The plasma jet generated by a torch module is described by the voltage-current characteristic of the discharge and through imaging of its plume in a quiescent environment and in a supersonic crossflow. This torch system, with its high voltage discharge, can be operated in periodic (60-Hz) or pulsed modes, depending on the power supply used. In the 60-Hz mode as presented in this work, the capacitors are charged at the line frequency of 60 Hz, resulting in a cyclical discharge. In this mode, the cycle energy is up to 46 J. However, this energy is mainly limited by the

power handling capability of the power supply. Within the Mach-2.5 supersonic flow, which approximates the supersonic-combustor startup condition (vis-à-vis the crossflow velocity), the penetration height and the volume of torch plume into the crossflow vs. gas supply pressure and plasma energy are determined.

As a consequence of the high-voltage nature of the discharge, the arc loop can be many times the distance between the anode and cathode. This is illustrated with the instantaneous image in Fig. 3.5.1, which was recorded with an intensified CCD camera (a Roper Scientific PIMAX) set for an 80 ns exposure time. The current loop is coincident with the thin, intense emission loop shown in the figure. For this measurement, pure nitrogen with pressure of 1.7 atm was supplied to the torch module. The distance between the cathode (at the center of the base line) and anode spot (on the left-hand side of the cathode) is about 7.5 mm, whereas the vertical extent of the arc loop is about 5 cm. Such an extended arc loop increases the path length of the charge particles in the discharge by more than 15 times the direct path length from the cathode to the anode spot. It has the advantages of improving 1) the lifetime of plasma (by reducing the transit time loss), 2) the lifetime of the electrodes (by reducing charge particles' kinetic energy before hitting electrodes), and 3) the conversion of electrical energy to plasma energy. Note also that images such as this one indicate that while the length of the arc loop is not strongly sensitive to the flow rate, the width of the loop becomes narrower as the flow rate increases. This is consistent with the change in the flowfield structure as the jet becomes underexpanded and supersonic with increased supply pressure.

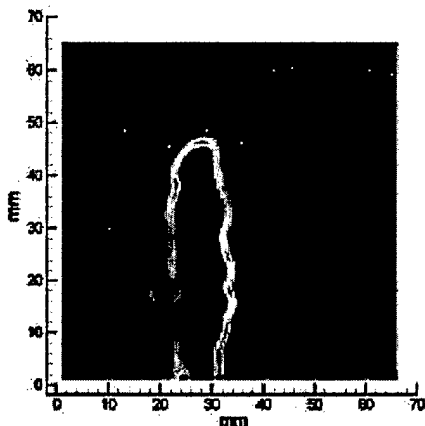


Fig. 3.5.1. Planar image of an arc loop in torch plasma taken by an intensified CCD camera with an 80-ns exposure. The diffuse emission surrounding the arc loop is from NO laser-induced fluorescence.

Figure 3.5.1 also shows a less intense laser-induced fluorescence (LIF) from nitric oxide, NO. The LIF is best seen in the background on the left side of the figure towards the outer portion of the arc loop. NO is produced within the torch plume in the region where the hot torch gas—particularly that gas near the arc—mixes with air. Thus, NO is formed primarily near the outer-portion of the arc loop. Here, we employed a Nd :YAG-pumped dye laser system to generate laser radiation at 226 nm and couple to the overlapped $Q_1(12.5)$ and $Q_2(19.5)$ transitions in the $\delta(0,0)$ band of NO.

The time varying voltage V and current I of the discharge was measured using a digital oscilloscope (Tektronix TDS3012 DPO 100 MHz and 1.25 GS/s) for each supply pressure p_0 in the range from 1.2 atm to 7.6 atm. Presented in Fig. 3.5.2a is a V-I characteristic plot from the results obtained in the case with the supply pressure of 6.67 atm. As shown, discharges are in the arc mode in both half cycles. In addition, significant hysteresis effects are observed in the half cycle when the central electrode is positive. The asymmetry of the V-I curve is due to the physical difference between the electrodes. The applied electric field concentrates in the region near the central electrode due to the cylindrical geometry, and this is where the discharge normally initiates. When the central electrode is positive, it collects electrons produced by the discharge. The transit-time loss of electrons increases the breakdown voltage considerably. After the discharge starts, it evolves quickly to the high-current low-voltage arc mode. In this regime the breakdown voltage drops dramatically to a value determined by recombination/attachment losses, rather the transit-time loss. It is the transition of the breakdown voltage during the discharge from transit-time losses to recombination/attachment losses that bifurcates the V-I relation to form the hysteresis loop shown on the right hand side of Fig. 3.5.2a. In the reverse cycle, the ring electrode collects electrons resulting in an insignificant transit time loss. In this case, the breakdown voltage is mainly determined by the recombination/attachment losses in the entire discharge period. This mechanism could explain the smaller hysteresis loop on the left-hand side of Fig. 3.5.2a.

The product of the V and I functions gives the instantaneous power function. The result in one cycle is presented in Fig. 3.5.2b. As shown, the one having a larger peak of about 8 kW is the power function of the discharge lasting about 5 ms with the diode in the circuit forward biased. In the reverse bias phase, the discharge lasts longer at about 6

ms, but the peak power is reduced to 5 kW. The average power of the torch over one cycle exceeds 2.7 kW. It is noted that the added diode in the circuit serves to reduce the voltage requirement of the transformer output for reliable discharge.

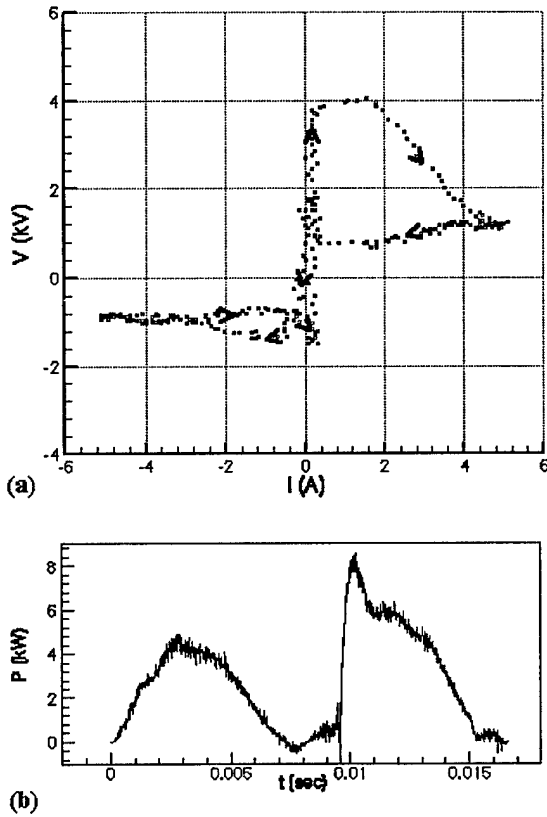


Fig. 3.5.2 (a) The V-I characteristic of the discharge in one cycle, and (b) the instantaneous power function $P = VI$.

Integrating the power function over one cycle determines the cycle energy of the torch, i.e., the thermal energy carried by torch plasma in each cycle. The results show that this cycle energy varies with the pressure p_0 . The dependence is presented in Fig. 3.5.3. As shown, in the regime of subsonic flow, the cycle energy increases to the maximum of about 28 J at $p_0 = 2.4$ atm. It increases again in the supersonic flow regime and reached the maximum of about 46 J at $p_0 = 6.4$ atm. The transition of the flow property from subsonic to supersonic results to a dip at $p_0 = 3$ atm in the plot. Excluding the dependence in the region $2 < p_0 < 3$ atm, the cycle energy of the torch increases with the increase of the flow rate (i.e., the supply pressure p_0 of the module) before reaching the largest peak located in the region $5.4 \leq p_0 \leq 6.4$. The increasing dependence of the plasma energy on the flow rate in the region of lower pressure (i.e., $p_0 \leq 6.4$ atm) is realized because the

supplied gas flow works to increase the transit time of charge particles by keeping the discharge away from the shortest (direct) path between two electrodes. As the flow rate increases, the transit time loss of charge particles is reduced. An increase of the current path also tends to increase the effective resistance in the discharge. Thus the discharge voltage increases, as observed in the forward bias phase. Consequently, the plasma energy increases. However, when the flow rate becomes too high (i.e., $p_0 > 6$ atm), the mobility of charge particles crossing the flow becomes significantly affected by the flow. It reduces the discharge current, which leads to the decreasing dependence of the torch energy on the pressure for $p_0 > 6$ atm.

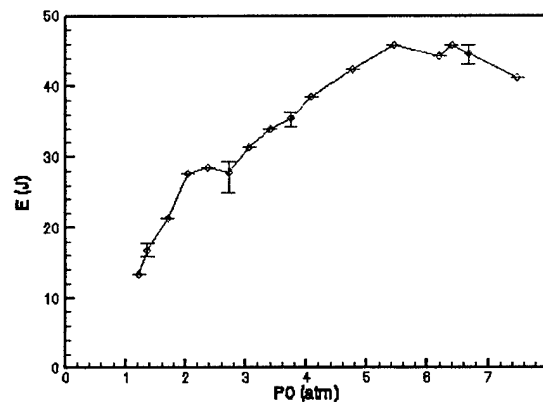


Fig. 3.5.3 The dependence of the cycle energy E of the torch plasma on the backpressure.

In summary, we have significantly improve the performance of the modular plasma torch—which alone, or in an assembly of torches—is intended as an ignition aid for a hydrocarbon-fueled scramjet engine. Two principal advantages of this torch module are 1) that it is a compact design based on conventional components and 2) that it is durable running for long periods of time with an air feedstock (but no addition cooling). The peak and average power can reach 8 kW and 2.8 kW, respectively, and the maximum cycle energy is 46 J. The other notable features of the plasma torch design particularly relevant to the intended application are 1) the relatively large gap between electrodes, resulting in a high-voltage discharge, and 2) the ceramic insulator inserted between the electrodes, allowing the discharge to take place outside the module. As a consequence of these design features, this torch module produces plasma directly in the open region,

maximizing the plasma gas feedstock interaction volume. These features are different from discharges produced in conventional non-transferred dc plasma torches. Excellent penetration of the plasma torch plume into a Mach 2.5 crossflow was demonstrated in early work. This aspect is important for supersonic combustion applications where injection and mixing are critical issues.

6. Conditions and a physical mechanism for plasma mitigation of shock wave in a supersonic flow

Wind tunnel experiments show that plasma generated by on-board discharges can significantly weaken the shock wave generated in front of a 30° half-angle truncated-cone model placed in a Mach 2.5 flow. Experimental results indicate that significant plasma effect on shock wave appeared only when two conditions: 1. plasma was generated in the region upstream of the baseline shock front and 2. plasma had a symmetrical spatial distribution with respect to the axis of the model, were met. Experimental results also exclude the thermal effect as a possible cause of the observed shock wave mitigation. A physical mechanism of the observed nonthermal plasma effect on shock waves is discussed. Analysis shows that a symmetrically distributed plasma spike in front of the shock as shown in Fig. 3.6.1 can effectively deflect the incoming flow symmetrically. The required electron density of the plasma spike is estimated.

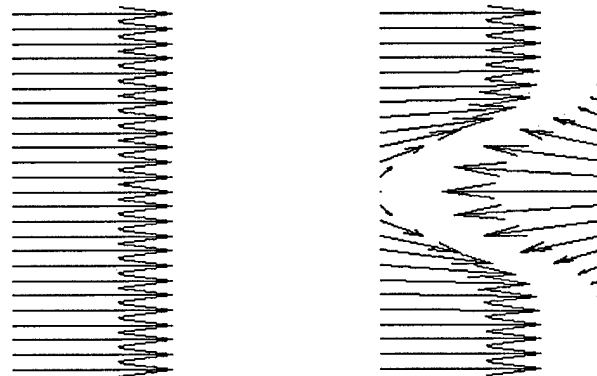


Fig. 3.6.1 Flux distributions of the incoming flow (left), the deflected flow (middle), and the electron flow (right) representing a plasma spike. x and y axes are in the horizontal and vertical directions

7. Characteristics of an arc-seeded microwave plasma torch

The design and operation of a portable microwave plasma torch is presented. An arc plasma torch running at 60 Hz and generated by a torch module, which is installed on the bottom wall in the narrow section of a tapered S-band rectangular cavity, is used to seed the microwave discharge at the location, where the microwave electric field is the maximum. This tapered cavity is designed to support TE_{103} mode. With seeding, only low Q cavity and moderate microwave power (time average power of 700 W) are needed. This torch can be run without applying a gas flow to stabilize the arc discharge and a large portion of microwave plasma can still be generated outside the cavity. Without a gas flow, the torch module works the same as a surface gap spark plug, which produces very small size seeding plasma near the bottom wall of the cavity. However, when the microwave is introduced, sizable torch plasma with a height of about 15 mm and a volume of about 3.5 cc outside of the cavity is generated as demonstrated in Fig. 3.7.1a. Introducing very small airflow (about 0.315 l/s) through the torch module can significantly increase the height (to about 25 mm) and the volume (to about 6 cc) of the torch plasma. A photo of this enlarged torch is presented in Fig. 3.7.1b for comparison. It is noted that in addition to the flow rate and microwave power, the size of this microwave torch plasma depends also on the size of the exit hole on the cavity wall. By doubling the diameter of the exit hole from 12.5 mm to 25 mm, the torch plasma can achieve a height more than 60 mm outside the cavity. However, the microwave leakage also exceeds the standard safety level, which is undesirable for a portable device. Further enlarging the exit hole will only reduce the size and volume of the torch because of the degradation of the Q-factor of the cavity.

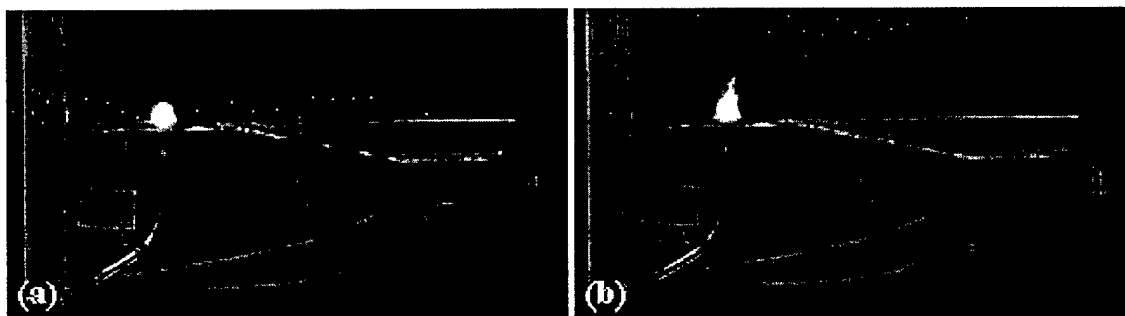


Fig. 3.7.1. Microwave torches (a) without flow and (b) with very low airflow.

The microwave-enhanced discharge increases the size, cycle energy, and duty cycle of the torch plasma considerably. This torch can be run without introducing gas flow to stabilize the arc and microwave discharges. Adding gas flow can increase not only the size of the torch plasma but also its cycle energy, which reaches a plateau of about 12 J/per cycle for gas flow rate exceeding 0.393 ℓ/s . The electron density and excitation temperature, and the composition of torch species are determined by emission spectroscopy. It is shown that, at the bottom of the torch close to the cavity wall, electrons distribute quite uniformly across the core of the torch with density and excitation temperature determined to be about $7 \times 10^{13} \text{ cm}^{-3}$ and 8000 K, respectively. It is also found that this torch produces an abundance of reactive atomic oxygen as evidenced by the emission spectroscopy of the torch presented in Fig. 3.7.2.

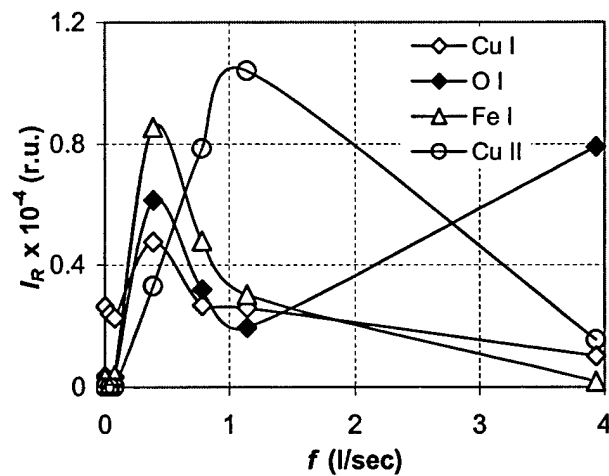


Fig. 3.7.2 The dependency of relative intensities I_R of spectral lines - Fe I (385.991 nm), Cu I (809.263 nm), Cu II (766.47 nm), and O I (777.194 nm) at the location approximately 25 mm away from the nozzle exit of the torch module, on the air-flow rate f .

References

1. R. M. Gage, *Arc Torch and Process* (United States Patent No. US2858411, 1961).
2. E. Koretzky and S. P. Kuo, "Characterization of an atmospheric pressure plasma generated by a plasma torch array," *Phys. Plasmas*, vol. 5, no. 10, pp. 3774-3780, 1998.
3. S. P. Kuo, E. Koretzky, and L. Orlick, "Design and electrical characteristics of a modular plasma torch," *IEEE Trans. Plasma Sci.*, vol. 27, no. 3, pp. 752-758, 1999.
4. S. P. Kuo, E. Koretzky, and L. Orlick, *Methods and Apparatus for Generating a Plasma Torch* (United States Patent No. US 6329628 B1, 2001).
5. R. J. Vidmar, "On the Use of Atmospheric Pressure Plasmas as Electromagnetic Reflectors and Absorbers," *IEEE Trans. Plasma Sci.*, 18, 733, 1990.
6. T. Wagner, W. O'Brien, G. Northam, and J. Eggers, "Plasma torch igniter for scramjets," *J. Propulsion and Power*, vol. 5, no. 5, 1989.
7. G. Masuya, K. Kudou, T. Komuro, K. Tani, T. Kanda, Y. Wakamatsu, N. Chinzei, M. Sayama, K. Ohwaki, and I. Kimura, "Some governing parameters of plasma torch igniter/flamholder in a scramjet combustor," *J. Propulsion and Power*, vol. 9, no. 2, pp. 176-181, 1993.
8. L. S. Jacobsen, C. D. Carter, and T. A. Jackson, "Toward plasma-assisted ignition in scramjets," *AIAA Paper 2003-0871*, American Institute of Aeronautics and Astronautics, Washington DC, Jan. 2003.
9. S. P. Kuo, Daniel Bivolaru, Campbell D. Carter, Lance Jacobsen, and Skip Williams, "Operational Characteristics of a Periodic Plasma Torch", *IEEE Trans. Plasma Sci.*, 32 (1), 262-268, 2004.
10. S. P. Kuo, "Conditions and a physical mechanism for plasma mitigation of shock wave in a supersonic flow", *Physica Scripta*, 70, 161-165, 2004.